Journal of Electroceramics, 13, 15–22, 2004
© 2004 Kluwer Academic Publishers. Manufactured in The Netherlands.

Recent Developments on MOCVD of Ferroelectric Thin Films

YOHEI OTANI,* SOICHIRO OKAMURA & TADASHI SHIOSAKI

Graduate School of Materials Science, Nara Institute of Science and Technology (NAIST), 8916-5 Takayama-cho, Ikoma, Nara 630-0192, Japan

Submitted January 29, 2003; Revised December 9, 2003; Accepted January 7, 2004

Abstract. Ferroelectric Pb(Zr,Ti)O_3 thin films were fabricated by liquid delivery MOCVD using Pb$(DPM)_2$, Ti$(O\textit{i}Pr)_2(DPM)_2$ and Zr$(DIBM)_4$. The deposition rate of 12.3 nm/min was attained on 6-inch Pt/Ti/SiO_2/Si wafers at 550°C. The average and the deviation of twofold remanent polarization were 45.5 μC/cm^2 and ±6.4%, respectively, over the 6-inch wafer. Step coverage was improved from 44% to 90% by decreasing deposition temperature from 550 to 400°C although the deposition rate decreased by 60%. TiO_2 nanoparticles diffused to the surface of platinum bottom electrodes were effective as a seed to obtain 111 preferential oriented PZT thin films at the deposition temperature of 550°C. Iridium oxide bottom electrodes were reduced to metal ones by CO and/or H_2 gases generated by decomposition of precursors. Oxide materials seem to be not the best as bottom electrodes in liquid delivery MOCVD. A cocktail source consisted of Pb$(METHD)_2$, Ti(MPD)$(METHD)_2$ and Zr$(METHD)_4$ was also examined. PbPt$_x$ alloy phase existed in PZT films deposited at 500°C was disappeared by post-annealing at 600°C and the annealed film showed hysteresis properties with the $2P_r$ of 56 μC/cm^2 and the $2E_c$ of 181 kV/cm.

Keywords: liquid delivery, MOCVD, PZT, cocktail source, 6 inch wafer

1. Introduction

A ferroelectric random access memory (FeRAM) is a promising candidate for future mainstream memory devices because of some advantages, such as nonvolatility, high-speed operation, high-endurance, low-voltage operation and low-power consumption, compared with DRAMs, EEPROMs and FLASH memories [1]. Recently, many manufacturers have announced the development of high-density FeRAMs with capacities of 8-64 Mbits [2–6]. Metalorganic chemical vapor deposition (MOCVD) has attracted much attention as a key technology for mass production of such high-density FeRAMs. Ferroelectric Pb(Zr,Ti)O_3 (PZT) is one of promising candidates used in such high-density FeRAMs. A large number of studies have been made on the formation of PZT thin films by MOCVD [7–10]. We also reported the formation of PZT thin films by MOCVD using tetraethyl lead Pb$(C_2H_5)_4$ or triethylneopentoxy lead (TEPOL) as lead sources [11, 12]. However, it was difficult to use such lead sources in industry because they were toxic. Liquid delivery MOCVD generally uses liquid sources prepared by dissolving metal complexes such as β-diketon in a solvent [13]. This made possible the utilization of novel lead sources, such as lead dipivaloylmethnate Pb$(DPM)_2$, which are less toxic and have little vapor pressure at room temperature.

For high-density FeRAMs, good step coverage on three-dimensional structure is desired. Lowering of deposition temperature is also required for compatibility with the fabrication process of LSIs. High speed and uniform deposition on large size wafers may cut down a fabrication cost. Therefore, we are challenging the formation of homogeneous ferroelectric PZT thin films on large size wafers with good step coverage at low temperature at high deposition rate by liquid delivery MOCVD [14–17]. We are also examining cocktail sources in which some precursors are premixed to

*To whom all correspondence should be addressed. E-mail: o-youhei@ms.aist-nara.ac.jp

simplify a delivery system. This paper describes recent developments in our laboratory on the formation of PZT thin films by liquid delivery MOCVD.

2. Experimental

2.1. Precursors

At the beginning of this study, $Pb(DPM)_2$, $Ti(O\textit{i}Pr)_2(DPM)_2$ and $Zr(DPM)_4$ dissolved in tetrahydrofuran (THF) were used as precursors in the formation of PZT thin films. However, higher supplying rate was required for $Zr(DPM)_4$/THF to form PZT thin films because $Zr(DPM)_4$ was stable and had higher decomposition temperature than other precursors. Then, we have selected zirconium diisobutylylmethnate $Zr(DIBM)_4$ as a Zr-precursor.

$Pb(DPM)_2$, $Ti(O\textit{i}Pr)_2(DPM)_2$ and $Zr(DIBM)_4$ should be separately delivered from each bottle to a vaporizer because some reactions occur among these precursors and vaporization properties may change if they were premixed. This makes the delivery system complex. Therefore, we also examined a cocktail source prepared from methoxyethoxytetramethylheptanedionato (METHD)-based precursors. The cocktail source was prepared by mixing $Pb(METHD)_2$, Ti(MPD = methylpentanedioxide)$(METHD)_2$ and $Zr(METHD)_4$ dissolved in ethylcyclohexane (ECH). Precursors used in this study are summarized in Table 1.

2.2. Vaporization System

In the liquid delivery MOCVD, liquid sources consist of metal complexes and solvent are instantaneously vaporized in a vaporizer. In this situation, vaporizer pressure has a great influence on the vaporization of precursors. However, in conventional liquid delivery MOCVD systems, it is difficult to control the vaporizer pressure because the vaporizers are directly connected to reactors evacuated to low pressure. Then, we inserted a gasket with a small orifice between a vaporizer and a reactor. This made possible to control the vaporizer pressure independent of the reactor pressure by changing the flow rate of a carrier gas. The vaporizer pressure was adjusted to 500 and 240 Torr for precursors of the DPM system and the METHD system, respectively.

2.3. Deposition System

A reactor was evacuated to the pressure of 3–5 Torr by a mechanical booster pump and a rotary pump. The reactor pressure was adjusted by a feedback-controlled valve, which was equipped between the reactor and the pumps. Source gases were mixed with oxygen gas preheated to 270–280°C in a double layer structured showerhead with a diameter larger than 6 inch. The mixed gas was then blown onto the substrates heated to appropriate temperature by a pyrolyzed boron nitride (PBN) heater just in size as the 6-inch wafers (Advanced Ceramics International Corporation). The substrates were rotated at 5 rpm during the deposition. Typical deposition conditions are summarized in Table 2.

2.4. Evaluations

The crystal structure and the orientation of deposited PZT thin films were confirmed by X-ray diffraction reciprocal space mapping (XRD-RSM) (X'Pert PRO MRD, PANalytical). The reciprocal space mapping method is a strong tool for characterization of thin

Table 1. The precursor materials used in this study.

Chemical formula	Abbreviation	Melting Point (°C)	Boiling point (°C / mmHg)	State at R.T.
$Pb(C_{11}H_{19}O_2)_2$	$Pb(DPM)_2$	126–128	140/0.05	Solid
$Pb(C_{14}H_{25}O_4)_2$	$Pb(METHD)_2$	–	–	Solid
$Zr(C_{11}H_{19}O_2)_4$	$Zr(DPM)_4$	44–45	72/0.2	Solid
$Zr(C_9H_{15}O_2)_4$	$Zr(DIBM)_4$	270–	–	Solid
$Zr(C_{14}H_{25}O_4)_4$	$Zr(METHD)_4$	–	–	Viscous liquid
$Ti(O\text{-}\textit{i}C_3H_7)_2(C_{11}H_{19}O_2)_2$	$Ti(O\textit{i}Pr)_2(DPM)_2$	164	–	Solid
$Ti(C_6H_{12}O_2)(C_{14}H_{25}O_4)_2$	$Ti(MPD)(METHD)_2$	–	–	Viscous liquid

Table 2. Typical deposition conditions of PZT thin films.

	Multi bottles		Cocktail bottle	
Source materials				
Pb source	$Pb(DPM)_2$	0.05 mol/L	$Pb(METHD)_2$	0.033 mol/L
Zr source	$Zr(DIBM)_4$	0.10 mol/L	$Zr(METHD)_4$	0.040 mol/L
Ti source	$Ti(OiPr)_2(DPM)_2$	0.10 mol/L	$Ti(MPD)(METHD)_2$	0.020 mol/L
Solvent	THF		ECH	
Source flow rates	Pb	0.96 g/min	Cocktail	1.20 g/min
	Zr	0.17 g/min		
	Ti	0.41 g/min		
	THF	0.20 g/min		
Carrier gas flow rate	N_2	2.10 L/min	Ar	0.14 L/min
Oxidation gas flow rate	O_2	1.00 L/min	O_2	0.20 L/min
Vaporizer temperature		270°C		280°C
Vaporizer pressure		500 Torr		240 Torr
Reactor pressure		5 Torr		3 Torr
Substrate temperature		400, 550°C		500°C
Showerhead temperature		200°C		200°C
Pipe temperature		270°C		280°C

films with fiber texture [18]. The composition of deposited PZT thin films was estimated by X-ray fluorescence (MagiX PRO, PANalysical). Circular platinum top electrodes with a diameter of 0.1 mm were deposited on the surface of PZT thin films by rf-magnetron sputtering with a metal shadow mask, and the electrical properties of the films were measured by a ferroelectric material analyzer (TF-2000, Aixacct).

3. Results and Discussion

3.1. Deposition on 6-Inch Wafers

PZT thin films were deposited on 6-inch $Pt/Ti/SiO_2/Si$ wafers at 550°C for 30 minutes by liquid delivery MOCVD using $Pb(DPM)_2$, $Ti(OiPr)_2(DPM)_2$ and $Zr(DIBM)_4$. The average thickness of the film was 370 nm; the deposition rate of 12.3 nm/min was attained at a total supplying rate of 114 μmol/min. The deviation in the thickness was less than ±10% over the 6-inch wafer. The films were crystallized into perovskite PZT with 100/001 mixed orientations at all the points of the wafer. However, lead platinum alloy, $PbPt_x$ was formed at the peripheries in addition to PZT. The formation of $PbPt_x$ is sometimes observed in the deposition of PZT thin films on platinum bottom electrodes by MOCVD [17, 19]. We believe that carbon monoxide and/or hydrogen, CO and/or H_2, generated by the decomposition of precursors have an important role in the formation of $PbPt_x$ alloy. It seems that lead atoms generated by reduction of lead oxides reacted with platinum at the surface of bottom electrodes and formed $PbPt_x$ alloy.

The lead contents at peripheries were higher by 5–7% than those at the center while the zirconium and the titanium contents were almost constant at a Zr:Ti molar ratio of 30:70 over the 6-inch wafer. This excess lead was due to the formation of $PbPt_x$ at peripheries. The twofold remanent polarization $2P_r$ higher than 40 $\mu C/cm^2$ was attained all the points of the 6-inch wafer as shown in Fig. 1. The average and the deviation of $2P_r$ were measured to be 45.5 $\mu C/cm^2$ and ±6.4%, respectively, over the 6-inch wafer in spite of the formation of $PbPt_x$ at peripheries. Figure 2 shows hysteresis loops of the PZT film at the center of the 6-inch wafer. The well-saturated hysteresis loop with $2P_r$ of 45.5 $\mu C/cm^2$ and $2E_c$ of 130 kV/cm was observed at the initial state and the remanent polarization decreased only by 30% after the polarization reversal of 10^9 cycles.

3.2. Improvement of Step Coverage

PZT thin films were deposited on SiO_2/Si substrates with microholes and planar $Pt/Ti/SiO_2/Si$ substrates at the substrate temperature of 400 and 550°C. Step coverage was drastically improved from 44 to 90% with decreasing the substrate temperature from 550 to 400°C

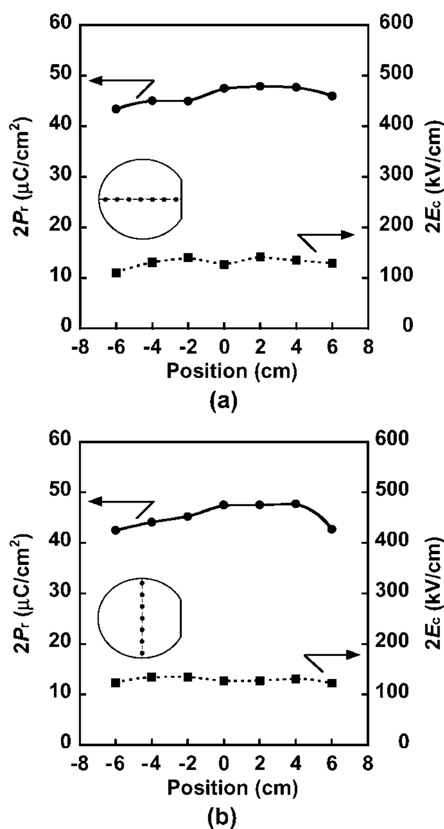

Fig. 1. The distribution of $2P_r$ on (a) the horizontal and (b) the vertical centerlines of the 6-inch wafers.

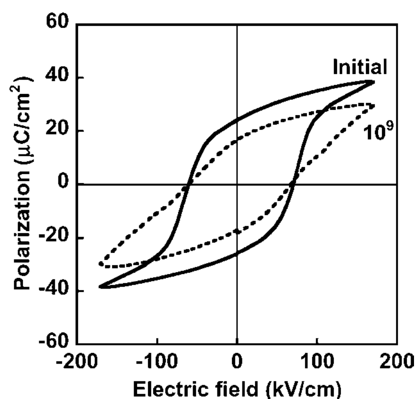

Fig. 2. Hysteresis loops of the PZT thin film at the center of the 6-inch wafers at initial state and after the polarization reversal of 10^9 cycles.

as shown in Fig. 3 while the deposition rate was reduced by 60%; from 10.4 to 4.0 nm/min. The Zr:Ti molar ratio was changed from 30:70 to 70:30 with decreasing the substrate temperature from 550 to 400°C. This means that the deposition efficiency of $Ti(O\textit{i}Pr)_2(DPM)_2$ was lower than those of $Pb(DPM)_2$ or $Zr(DIBM)_4$ at low temperature. A new titanium precursor which has lower decomposition temperature will be needed for low temperature deposition.

The PZT thin films deposited on $Pt/Ti/SiO_2/Si$ substrates at 400°C were amorphous and did not show any hysteresis properties while the films deposited at 550°C were crystallized into perovskite PZT. After the post-annealing at 600°C in air for 30 minutes, the films deposited at 400°C were crystallized into perovskite PZT and showed hysteresis properties.

We concluded that the combination of the deposition at low temperature and post-annealing at higher temperature is one of the solutions that make possible the fabrication of the ferroelectric PZT capacitors with excellent step coverage on three-dimensional structure.

3.3. Orientation Control of PZT Thin Films

PZT thin films formed by MOCVD at low temperature tend to have 100/001 mixed orientations although 111 oriented PZT thin films are desirable for high reliable FeRAMs. Therefore, a high temperature of 620°C is currently used in industry for the deposition of PZT thin films to obtain a 111 orientation [2]. Some seeding layer will be required for lowering deposition temperature in the near future. Therefore, we are examining suitable bottom electrode structure to obtain 111 oriented PZT thin films.

Two kinds of $Pt/TiO_2/SiO_2/Si$ substrates were prepared: one with a 200 oriented rutile TiO_2 layer and the other with a 103 oriented anatase TiO_2 layer. The rutile and anatase TiO_2 layers were formed by depositing metal titanium thin films at room temperature and annealed at 700 and 400°C in O_2, respectively. Platinum layers were deposited on the TiO_2 layers by rf-magnetron sputtering at 500°C. Both platinum layers deposited on two kinds of TiO_2 layers had 111 orientations. TiO_2 nanoparticles were observed on the surface of the platinum layer only in case of anatase [20]. PZT thin films were deposited on both substrates at 550°C. Figure 4 shows the volume fraction of each orientation perpendicular to the substrate surface calculated from XRD-RSM charts. The PZT thin film had a preferential 111 orientation in case of anatase TiO_2 while 100/001 mixed orientations were obtained in case of rutile TiO_2. This result suggests that TiO_2 is effective

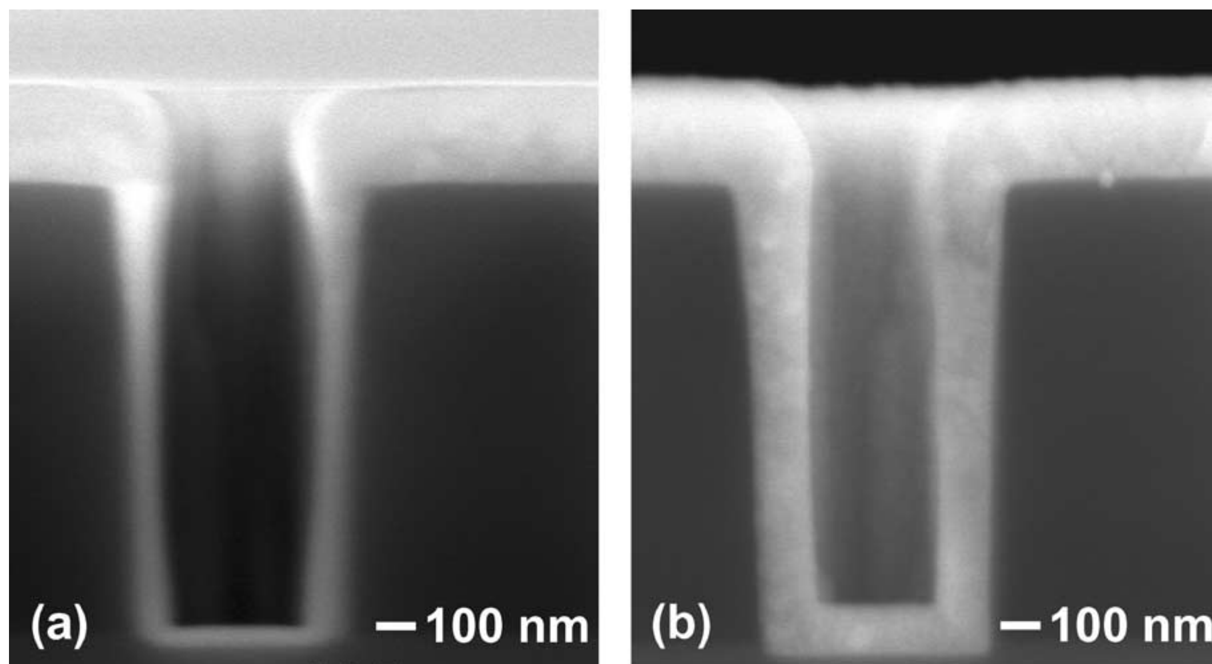

Fig. 3. Cross-sectional images of the PZT thin films deposited on SiO_2/Si substrates with microholes at (a) 550°C and (b) 400°C.

as a seed to obtain 111 oriented PZT thin films at low temperature.

3.4. *Deposition on IrO_2 Bottom Electrodes*

Some oxide electrodes such as IrO_2 [21] and $SrRuO_3$ [22] are useful to prevent the fatigue of PZT capacitors. Therefore, we examined the deposition of PZT thin films on IrO_2 bottom electrodes. IrO_2 thin films with a thickness of 20 nm were deposited on Pt/TiO_2/SiO_2/Si substrates by reactive sputtering at the substrate temperature of 400°C. Then, PZT thin films were deposited on the IrO_2 layers at 550°C. Figure 5 shows XRD-RSM charts of the samples before and after the PZT deposition. Some diffraction peaks due to IrO_2 were observed before the PZT deposition as shown in Fig. 5(a). However, these peaks disappeared and the diffraction peaks due to $PbPt_x$ alloy appeared in addition to PZT diffraction peaks after the PZT deposition as shown in Fig. 5(b). This means that the IrO_2 layer was reduced during the PZT deposition and lead atoms diffused to the platinum surface through grain boundaries of the reduced Ir, and then reacted with platinum as shown in Fig. 6. We concluded from these results that conductive oxide materials such as IrO_2 are not suitable for bottom electrodes in liquid delivery MOCVD.

3.5. *Deposition Using a Cocktail Solution*

A cocktail solution was prepared by mixing $Pb(METHD)_2$, $Zr(METHD)_4$ and Ti(MPD) $(METHD)_2$ at a Pb:Zr:Ti molar ratio of 1.65:2.00:1.00. PZT thin films were deposited on Pt/Ti/SiO_2/Si substrates at 500°C for 30 minutes using the cocktail solution. The thickness of deposited films was 390 nm; the deposition rate of 13 nm/min was attained at a total source supplying rate of 129 μmol/min. The Pb:Zr:Ti molar ratio of the deposited PZT films was estimated to be 1.55:0.33:1.00. It is found from these results that the depositing efficiency of the Zr precursor was approximately 1/6 of the Ti precursor at 500°C. The development of novel cocktail sources including a Zr precursor with high deposition efficiency is urgently required for low temperature deposition.

Figure 7 shows the XRD-RSM charts of the PZT films deposited at 500°C and subsequently annealed at 600°C. $PbPt_x$ alloy and lead oxide (PbO) were formed in addition to PZT in the as-deposited film as shown

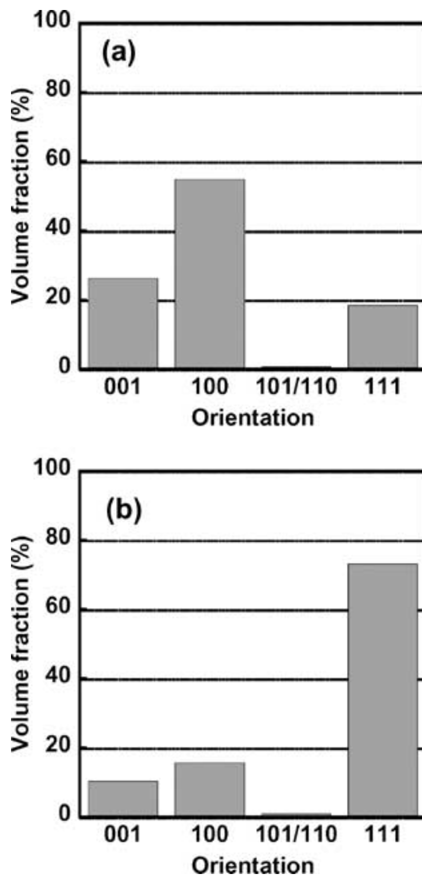

Fig. 4. Relative volume fractions of each orientation of the PZT thin films deposited on $Pt/TiO_2/SiO_2/Si$ substrates (a) without and (b) with TiO_2 nanoparticles on the surface of platinum bottom electrodes.

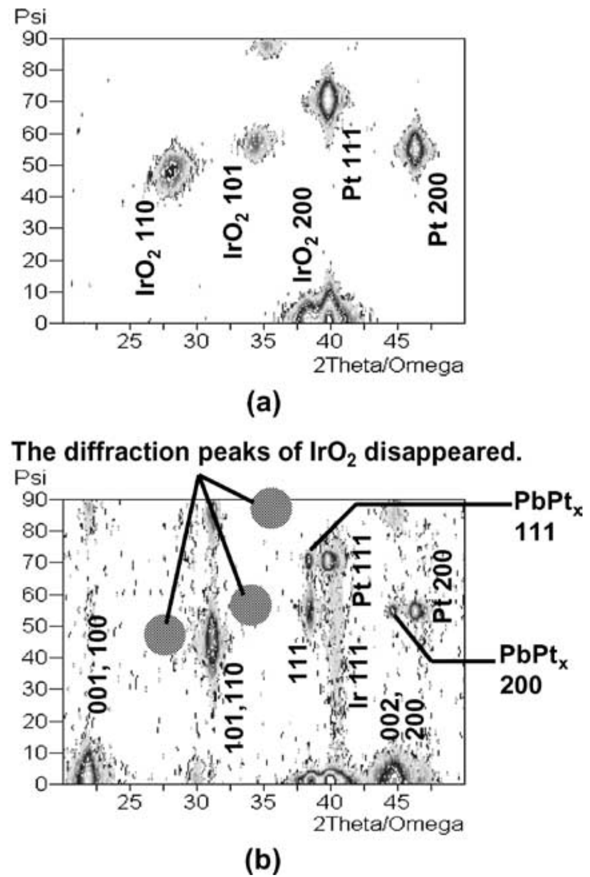

Fig. 5. XRD-RSM charts of $IrO_2/Pt/TiO_2/SiO_2/Si$ substrates (a) before and (b) after PZT deposition.

in Fig. 7(a). All these indexes were confirmed by the XRD-RSM measurement of wide scan range from 20 to 70 degree in 2theta. Pyrochlore phase was not observed in this film. The $PbPt_x$ alloy had a strong 111 orientation just like the platinum thin film while the PZT thin film had 100/001 mixed orientations. The existence of PbO indicated that the as-deposited film had excess lead atoms. The diffraction peaks due to $PbPt_x$ and PbO disappeared after the post-annealing at 600°C for 30 minutes in air as shown in Fig. 7(b). The $PbPt_x$ alloy was decomposed and oxidized at 450°C and the excess PbO was evaporated at 600°C. The as-deposited thin film without post-annealing after the deposition of platinum top electrodes showed the rounded hysteresis loops as shown in Fig. 8(a). The post-annealing at higher than 450°C improved hysteresis properties significantly and the capacitors annealed at 600°C showed well-saturated hysteresis loop as shown in Fig. 8(b), although the post-annealing at 400°C did not affect hysteresis properties. It seems that this improvement was not only due to the formation of the symmetrical contacts between ferroelectrics and electrodes but also the structural change of this films with disappearance of PbO and $PbPt_x$ phases. The twofold remanent polarization and the twofold coercive field of the annealed PZT film were 56 $\mu C/cm^2$ and 181 kV/cm, respectively.

4. Summary

Fabrication of ferroelectric PZT thin films by liquid delivery MOCVD was investigated from the applying point of view to the mass production of high-density FeRAMs. In the first half, $Pb(DPM)_2$, $Ti(OiPr)_2(DPM)_2$ and $Zr(DIBM)_4$ dissolved in THF

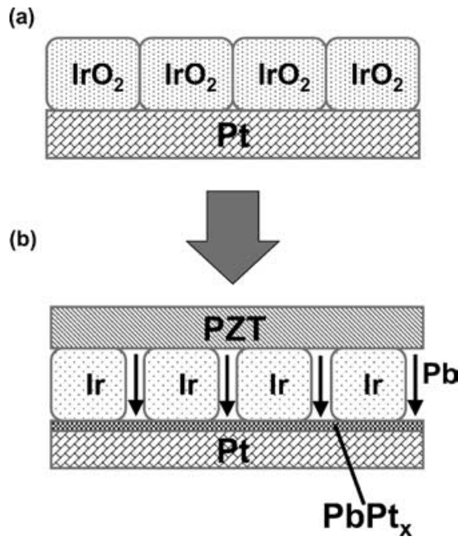

Fig. 6. Schematic diagram of the mechanism on the reduction of IrO_2 and the formation of $PbPt_x$ alloy.

were used as liquid sources. The deposition rate of 12.3 nm/min was attained on 6-inch $Pt/Ti/SiO_2/Si$ wafers at 550°C at a total source supplying rate of 114 μmol/min. The average and the deviation of twofold remanent polarization were 45.5 $\mu C/cm^2$ and 6.4%, respectively, over the 6-inch wafer. Step coverage of 90% was attained at 400°C although post-annealing at higher temperature was needed for crystallization into perovskite PZT. However, the deposition efficiency of $Ti(O\textit{i}Pr)_2(DPM)_2$ at 400°C was obviously lower than those of other sources. It is necessary to develop novel titanium sources with lower decomposition temperature for low temperature deposition. 111 preferential oriented PZT thin films were obtained even at 550°C by using TiO_2 nanoparticles diffused to the surface of bottom platinum electrodes as a seed. It is found that oxide materials are not the best for bottom electrodes in liquid delivery MOCVD because IrO_2 bottom electrodes were reduced to metal Ir. It seems that CO and/or H_2 gases generated by decomposition of precursors reduced the IrO_2 electrodes. Those CO and/or H_2 gases also caused the formation of $PbPt_x$ alloy.

In the latter part, we investigated on a cocktail source consisted of $Pb(METHD)_2$, $Ti(MPD)(METHD)_2$ and $Zr(METHD)_4$ dissolved in ECH. The PZT films deposited at 500°C using the cocktail source and annealed at 600°C showed hysteresis properties with the $2P_r$ of 56 $\mu C/cm^2$ and the $2E_c$ of 181 kV/cm. However,

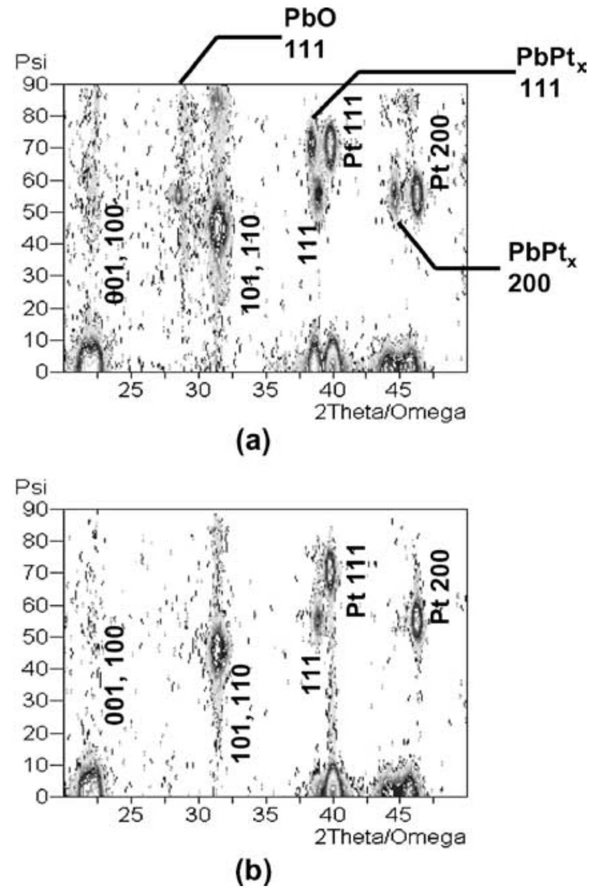

Fig. 7. XRD-RSM charts of the PZT thin films (a) deposited at 500°C using a cocktail source and (b) subsequently annealed at 600°C for 30 min.

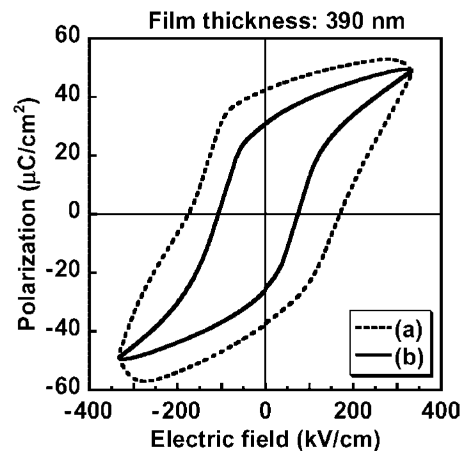

Fig. 8. Hysteresis loops of the PZT thin films deposited at 500°C using a cocktail source (a) and subsequently annealed at 600°C for 30 min (b).

the deposition efficiency of Zr-precursor was approximately 1/6 of that of Ti-precursors. The development of novel cocktail sources including a Zr precursor with high deposition efficiency is urgently needed.

References

1. H. Takasu, *J. Electroceramics*, **4**, 327 (2000).
2. Y. Horii, *NIKKEI ELECTRONICS*, 3rd March, 125 (2003) (in Japanese).
3. N. Nagano, T. Mikawa, T. Kutsunai, S. Hayashi, T. Nasu, S. Natsume, T. Tatsunari, T. Ito, S. Goto, H. Yano, A. Noma, K. Nagahashi, T. Miki, M. Sakagami, Y. Izutsu, T. Nakakuma, H. Hirano, S. Iwanari, Y. Murakuki, K. Yamaoka, Y. Goho, Y. Judai, E. Fujii, and K. Sato, in *2003 Symposium on VLSI Tech. Dig.* (Kyoto, Japan, 2003).
4. K. Oikawa, D. Takashima, S. Shiratake, K. Hoya, and O. Joachim, in *2003 Symposium on VLSI Tech. Dig.* (Kyoto, Japan, 2003).
5. S.R. Summerfelt, T.S. Moise, G. Xing, L. Colombo, T. Sakoda, S.R. Gilbert, A.L.S. Loke, S. Ma, L.A. Wills, R. Kavari, T. Hsu, J. Amano, S.T. Johnson, D.J. Vestcyk, M.W. Russell, S.M. Bilodeau, and P. van Buskirk, *Appl. Phys. Lett.*, **79**, 4004 (2001).
6. J.K. Lee, M.-S. Lee, S. Hong, W. Lee, Y.K. Lee, S. Shin, and Y. Park, *Jpn. J. Appl. Phys.*, **41**, 6690 (2002).
7. H. Fujisawa, K. Kita, M. Shimizu, and H. Niu, *Jpn. J. Appl. Phys.*, **40**, 5551 (2001).
8. M. Aratani, K. Nagashima, and H. Funakubo, *Jpn. J. Appl. Phys.*, **40**, 4126 (2001).
9. S.R. Summerfelt, T.S. Moise, G. Xing, L. Colombo, T. Sakoda, S.R. Gilbert, A.L.S. Loke, S. Ma, L.A. Wills, R. Kavari, T. Hsu, J. Amano, S.T. Johnson, D.J. Vestcyk, M.W. Russell, S.M. Bilodeau, and P. van Buskirk, *Appl. Phys. Lett.*, **79**, 4004 (2001).
10. J.K. Lee, M.-S. Lee, S. Hong, W. Lee, Y.K. Lee, S. Shin, and Y. Park, *Jpn. J. Appl. Phys.*, **41** 6690 (2002).
11. M. Shimizu, H. Fujisawa, M. Sugiyama, and T. Shiosaki, *Jpn. J. Appl. Phys.*, **33**, 5135 (1994).
12. M. Shimizu, S. Hyodo, H. Fujisawa, H. Niu, and T. Shiosaki, *Jpn. J. Appl. Phys.*, **36**, 5808 (1997).
13. T. Kawahara, M. Yamamuka, T. Makita, K. Tsutahara, A. Yuuki, K. Ono, and Y. Matsui, *Jpn. J. Appl. Phys.*, **33**, 5897 (1994).
14. M. Miyake, K. Lee, S. Okamura, and T. Shiosaki, *Integrated Ferroelectrics*, **36**, 127 (2001).
15. M. Miyake, K. Lee, S. Kawasaki, Y. Ueda, S. Okamura, and T. Shiosaki, *Jpn. J. Appl. Phys.*, **41**, 241 (2002).
16. Y. Ueda, N. Abe, Y. Otani, M. Miyake, S. Okamura, and T. Shiosaki, *Integrated Ferroelectrics*, **46**, 125 (2002).
17. Y. Otani, N. Abe, Y. Ueda, M. Miyake, S. Okamura, and T. Shiosaki, *Integrated Ferroelectrics*, **51**, 63 (2003).
18. K. Saito, T. Kurosawa, T. Akai, T. Oikawa, and H. Funakubo, *J. Appl. Phys.*, **93**, 545 (2003).
19. H.R. Kim, S. Jeong, C.B. Jeon, O.S. Kwon, and C.S. Hwang, *J. Mater. Res.*, **16**, 3583 (2001).
20. N. Abe, Y. Otani, M. Miyake, M. Kurita, H. Takeda, S. Okamura, and T. Shiosaki, *Jpn. J. Appl. Phys.*, **42**, 2791 (2003).
21. T. Nakamura, Y. Nakao, A. Kamisawa, and H. Takasu, *Appl. Phys. Lett.*, **65**, 1522 (1994).
22. C.B. Eom, R.B. Van Dover, J.M. Phillips, D.J. Werder, J.H. Marshall, C.H. Chen, R.J. Cava, and R.M. Fleming, *Appl. Phys. Lett.*, **63**, 2570 (1993).